

Received: 9 November 2007,

Revised: 8 July 2008,

Accepted: 17 July 2008,

Published online in Wiley InterScience: 1 October 2008

(www.interscience.wiley.com) DOI 10.1002/poc.1432

Photocatalytic TiO_2 – assisted decomposition of Triton X-100: inhibition of *p*-nitrophenol degradation

Gloria Pardo^a, Ronald Vargas^a and Oswaldo Núñez^{a*}



A decrease in the apparent pseudo first-order rate constant is observed in the photocatalyzed (TiO_2) degradation of surfactant Triton X-100 (Triton) when its concentration is increased. The measured rate *versus* the concentration profile is consistent with a hyperbolic form (rate increases with concentration) as described by the Langmuir–Hinshelwood (L–H) model. The rate is then given by the expression: $r = kK[\text{Triton}] / (1 + K[\text{Triton}])$ but the apparent rate constant by $k_{\text{app}} = kK / (1 + K[\text{Triton}]_0)$, where $k = 0.66 \text{ mg L}^{-1} \text{ min}^{-1}$ and $K = 0.037 \text{ L mg}^{-1}$. Therefore, at low $[\text{Triton}]_0$, $k_{\text{app}} = kK$ but at high $[\text{Triton}]_0$, $k_{\text{app}} = k / [\text{Triton}]_0$, that is, an inverse function of the reactant concentration. Although, in the latter case the reaction does not follow first-order kinetics, its pseudo first-order deviation is not easily noticeable. Therefore, this decrease in k_{app} with reactant concentration may limit its use when rate constants are compared to evaluate degradation efficiency or when it is used to show reaction inhibition. However, we have detected *p*-nitrophenol inhibition induced by Triton using k_{app} values. Inhibition is observed at $[\text{Triton}]_0 < \text{CMC}$ (critical micelle concentration) and also at $[\text{Triton}]_0 > \text{CMC}$. These inhibitions are consistent with the LH model given by the expression: $r = k'K'[\text{phenol}] / (1 + K'[\text{phenol}]_0 + K[\text{Triton}]_0)$, where $[\text{phenol}]$ is equal during all kinetic runs.

Copyright © 2008 John Wiley & Sons, Ltd.

Supporting information may be found in the online version of this article.

Keywords: photocatalysis; TiO_2 ; Triton X-100; apparent rate constant; *p*-nitrophenol

INTRODUCTION

The process of heterogeneous photocatalysis using TiO_2 is one of the so-called advanced oxidation processes (AOPs) that show promise for complete removal of organic compounds from contaminated waters. In these processes the produced hydroxyl radicals efficiently promote the oxidation of organic pollutants.^[1,2] The technology appears quite attractive since solar radiation energy is used to initiate the degradation (solar detoxification).^[3]

Various studies^[4] have demonstrated the efficiency of the TiO_2 /UV process in the mineralization of organic chlorides, carboxylic acids, unsaturated, and aromatic compounds. We have recently found^[5] TiO_2 photoinduced degradation and mineralization of some pesticide/fungicide precursors. Surfactants have also been studied due to their associated low biodegradability. These compounds are extensively used in the domestic and industrial fields therefore, their environmental impact on waters is quite important. It has been reported^[6–9] that anionic, cationic, and nonionic surfactants can be degraded using TiO_2 /UV.

Soil and underground water contamination by Non Aqueous Phase Liquids (NAPL) are also potential targets for solar detoxification. Decontamination involves a pump and treatment process. However, due to accumulation of the NAPL (especially the dense ones; DNAPL) at the soil pores, desorption becomes inefficient.^[10,11] However, using surfactants at concentrations higher than the critical micelle concentration (CMC), the water

solubility of the hydrophobic compounds increases.^[12,13] Therefore, extraction with surfactants has been proposed as an alternative for NAPLs recovery from contaminated underground waters and soils.^[10,11,14,15] Nonionic surfactants have been shown to be more effective in the solubilization and extraction of organic contaminants.^[16] Surfactant solution is introduced into the contaminated underground zone and then removed by pumping to a treatment tank where the extracted contaminant may be treated using TiO_2 /UV technology. Once the contaminant is eliminated, the micelle solution is separated using ultra filtration or flotation.^[17]

From petroleum production to its refining, we could find pits and effluents that require treatment due to the water or sediment contamination by hydrocarbons. Therefore, evaluation of the surfactant degradation and the influence of its concentration on the organic contaminant degradation are required in order to optimize treatment conditions. In fact, we have been working at

* Correspondence to: O. Núñez, Laboratorio de Fisicoquímica Orgánica y Química Ambiental, Departamento de Procesos y Sistemas, Universidad Simón Bolívar, Apartado Postal 89.000, Caracas, Venezuela.
E-mail: onunez@usb.ve

a G. Pardo, R. Vargas, O. Núñez
Laboratorio de Fisicoquímica Orgánica y Química Ambiental, Departamento de Procesos y Sistemas, Universidad Simón Bolívar, Apartado Postal 89.000, Caracas, Venezuela

laboratory level on this matter.^[18] In general, the mechanism of TiO₂ photodegradation can be explained^[2,19–22] using the Langmuir–Hinshelwood (L-H) model. However, details on the mechanism are still under investigation.^[23–27]

The value of the limiting degradation rate (k) (also known as the apparent Langmuir–Hinshelwood (L-H) rate constant) and the adsorption–desorption equilibrium constant (K) of L-H model under different experimental conditions, are quite important for optimizing the photocatalytic degradation. For instance, we have found^[28] selective TiO₂ photodegradation of naphthalene in Triton solutions. However, the use of rate constants must be considered with care since there is evidence^[21,29] that the pseudo first-order rate constant measured depends on reactant concentration. In this work, kinetic results on the degradation of surfactant Triton (*tert*-octylphenoxy polyethoxy-ethanol) using disperse TiO₂ and simulated solar light are shown. We studied the effect of the initial surfactant concentration and pH on the measured apparent pseudo first-order rate constant. Mineralization was also followed by means of OCD (oxygen chemical demand) measurements. Additionally, we studied the influence of Triton at different concentrations on the degradation of *p*-nitrophenol. We did not focus on the mechanism of *p*-nitrophenol degradation, since several proposals^[30–33] have been published on phenol degradation where dihydroxy phenol is one of the formed intermediates. We focus on the valid use of the rate constant as a parameter to evaluate the efficiency and competition between two degradable species when the TiO₂/UV process is used. From the mechanistic point of view, we also investigated on the degradation and mineralization of Triton. Therefore, a degradation path based upon kinetics and detected intermediates is proposed.

EXPERIMENTAL SECTION

Materials, equipment, and general procedures

Anatase, 99.9% TiO₂ was obtained from ALDRICH; Triton from SHARLAU and *p*-nitrophenol, spectrophotometric grade, from SIGMA. The K₂Cr₂O₇ and H₂SO₄ used to determine OCD as well as the H₃PO₄, KOH, and anhydrous sodium sulfate were obtained from RIEDEL DE HAEN.

Irradiations were conducted using a solar light simulator from SOLAR LIGHT Co. Model LS 1000 UV equipped with a Xenon lamp of 1000 W and filters that simulate solar light intensities in the UVB and UVA (290–400 nm). Radiation intensity was measured with a radiometer from SOLAR LIGHT Co. model PMA 2100. Kinetics were followed using a diode array HEWLETT PACKARD (HP) UV-visible spectrophotometer, MODEL 8452 A. Solutions of *p*-nitrophenol and Triton were prepared by adding KH₂PO₄ (final concentration: 0.001 M) and adding KOH (0.5 M solution) until the final pH (7 and 10) was obtained. By adding H₃PO₄ 0.01 M and using KOH 0.5 M, a final pH 4, was obtained. Irradiations were performed in a 4 L beaker using 1 L of solution and a TiO₂ suspension of 100 mg L⁻¹. The mixture was magnetically stirred during irradiation. Previous to irradiation, the reaction mixture was stirred in darkness for 30 min. During the reaction, sample aliquots were taken at different times from the reactor and filtered through a 0.45 μ m membrane to separate the TiO₂.

Photodegradation at different Triton initial concentrations

The initial [Triton] were in the range 24.8–124 mg L⁻¹. The experiments were run at pH 7. Kinetics were followed at 225 nm. A

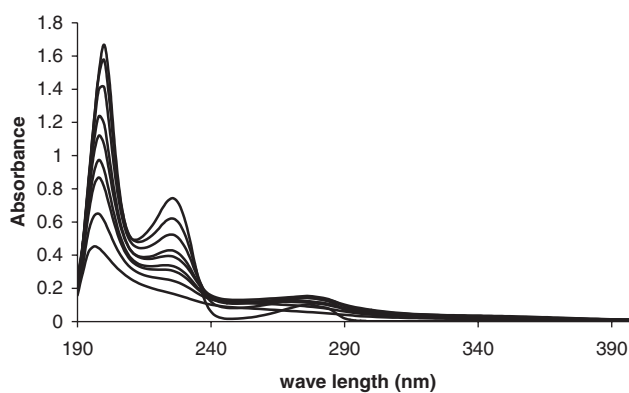


Figure 1. Triton–water solution UV spectra at different photodegradation times at 22 °C. Solar light simulator UVB and UVA (290–400 nm), light intensity 50 μ W cm⁻², [Triton]₀ = 48.8 mg L⁻¹, pH 7 and 100 mg L⁻¹ of Anatase 99.9% TiO₂ suspension. Reaction time (top to bottom): 0, 15, 30, 45, 60, 75, 90, 120, and 180 min

calibration curve (Absorbance vs. concentration) was previously obtained under the same reaction conditions. An absorptivity at 225 nm of $0.0144 \pm 0.0003 \text{ L cm}^{-1} \text{ mg}^{-1}$ ($9086 \text{ M}^{-1} \text{ cm}^{-1}$, when a Triton MW average of 631 is used) was obtained. Therefore, In [Triton] versus t plots was used to evaluate the apparent (k_{app}) pseudo first-order rate constants of degradation. In Fig. 1 a typical kinetic run at pH 7, [Triton]₀ = 48.8 mg L⁻¹ is shown.

pH influence

Triton degradation was followed at pH 4, 7, and 10 using a [Triton]₀ of 48.8 mg L⁻¹ and a TiO₂ suspension of 100 mg L⁻¹.

Mineralization

Triton mineralization was followed by measuring at each time the OCD. OCD was measured by titration with chromic acid.^[34,35]

Intermediates identification

Four intermediates were formed during photocatalytic degradation of 48.8 mg L⁻¹ of Triton at pH 4, irradiation intensity 50 μ W cm⁻² and [TiO₂] 100 mg L⁻¹. These intermediates were identified by GC/MS. The previously filtered irradiated samples (1 L) were acidified (H₂SO₄) to pH 2 and extracted with 30 ml of dichloromethane. The extracted were filtered on anhydrous sodium sulfate (twice). The solvent was evaporated at environment temperature to a final 1 ml volume. This solution was directly injected into a GCMS (Hewlett Packard, HP), model HP6890, provided with mass detector HP5973. The following injection conditions were used: HP-5 column 30 m \times 0.32 μ m internal diameter; eluent gas He; flux 38.1 ml min⁻¹; injection temperature 240 °C; column temperature at 40 °C during 4 min and 40–300 °C at 10 °C min⁻¹.

Photocatalytic degradation of *p*-nitrophenol in Triton solutions

The surfactant concentration influence on the *p*-nitrophenol photocatalytic degradation was studied under the following conditions: a fixed 13.7 mg L⁻¹ initial [p-nitrophenol]₀ was used while changing the initial [Triton] to 53.2, 106.4, 150, 212.1, and 319.2 mg L⁻¹. The pH was kept constant at 7. Degradation was

followed at 402 nm using previously prepared calibration curves (Absorbance vs. $[p$ -nitrophenol], $\epsilon = 9702 \text{ M}^{-1}$ at 402 nm). Apparent rate constants (k'_{app}) were obtained from $\ln [p\text{-nitrophenol}]$ versus t plots.

RESULTS AND DISCUSSION

Triton degradation

As shown in Fig. S1 (Supporting information) there is no observable degradation of Triton under conditions of absence of light with TiO_2 or absence of TiO_2 with simulated solar light. However, degradation is observed under conditions in which both, simulated solar light and TiO_2 are present. The linear plots of $\ln [\text{Triton}]$ versus t obtained are shown in Fig. 2. Apparent pseudo first-order rate constants were obtained from the slopes of these lines. As observed in Fig. 2, the slope decreases with concentration. It has been shown^[36,37] that the photocatalytic (TiO_2) degradation of organic water contaminants follows Langmuir–Hinshelwood (L-H) rate form given by

$$\text{rate} = \frac{kK[\text{Triton}]}{1 + K[\text{Triton}]} = k_{\text{app}}[\text{Triton}] \quad (1)$$

Where K (L mg^{-1}) corresponds to the proportion of Triton molecules which adhere to the surface of the TiO_2 particles, k ($\text{mg L}^{-1} \text{ min}^{-1}$) the limiting degradation rate at maximum coverage of the adsorbed Triton and $[\text{Triton}]$ (mg L^{-1}) the concentration of Triton. In fact, as predicted from Eqn (1), a plot of $1/\text{rate}$ versus $1/[\text{Triton}]_0$ (Fig. 3) is linear (rates obtained from initial rate measurements). From this plot and the intercept, a value for $k = 0.66 \pm 0.07 \text{ mg L}^{-1} \text{ min}^{-1}$ is obtained and from the slope, a value of $K = 0.037 \pm 0.008 \text{ L mg}^{-1}$ is obtained. From best fitting of the experimental points to Eqn (2), a $k = 0.80 \text{ mg L}^{-1} \text{ min}^{-1}$ and a $K = 0.06 \text{ L mg}^{-1}$ are also obtained (Fig. 4). Photocatalytic degradation of the surfactant Triton proceeds then through the L-H reaction mechanism, where a pre-equilibrium (K) between the amount of adsorbed Triton on the TiO_2 surface and the concentration in solution is established. The adsorbed Triton is further oxidized at the TiO_2 near surface either directly by the positive holes (h^+) at the TiO_2 valence band (formed by the

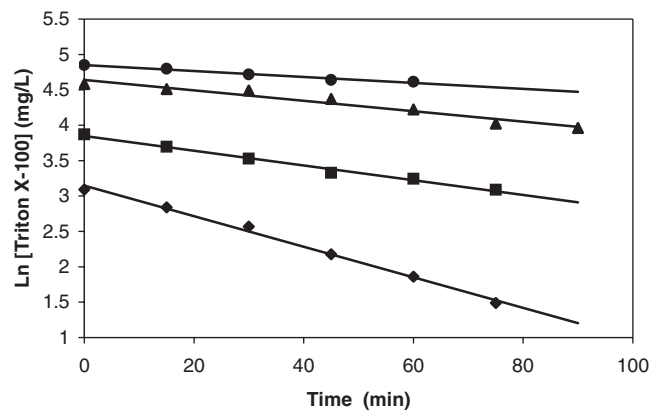


Figure 2. Effect of the initial $[\text{Triton}]$ on the slope of the $\ln [\text{Triton}]$ versus time plots. Radiation intensity $50 \mu\text{W cm}^{-2}$, $[\text{TiO}_2] 100 \text{ mg L}^{-1}$, pH 7 (water), temperature 22°C . From top to bottom $[\text{Triton}]_0$: 124, 99, 48.8, and 24.8 mg L^{-1}

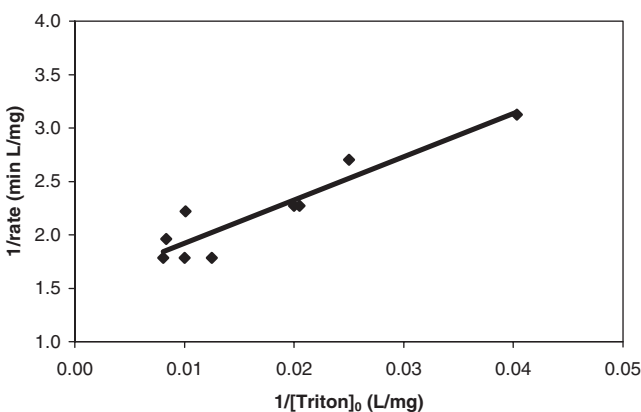


Figure 3. Langmuir–Hinshelwood plot ($1/\text{rate}$ vs. $1/[\text{Triton}]_0$) for Triton degradation. Radiation intensity $50 \mu\text{W cm}^{-2}$, $[\text{TiO}_2] 100 \text{ mg L}^{-1}$, pH 7 (water), temperature 22°C

UV-light excitation of an electron at the valence band into the conduction band)^[2] or by the action of hydroxyl radicals.^[21,22]

In Table 1 (second column), the experimental k_{app} values are shown. In the fourth and fifth columns the theoretical k_{app} values obtained from the k and K values from Fig. 3 and best fitting (Fig. 4) using in both cases Eqn (2) (as in Eqn (1)) are also shown

$$k_{\text{app}} = \frac{kK}{1 + K[\text{Triton}]_0} \quad (2)$$

As shown in Table 1 (R^2 values, third column) and Fig. 2, the Triton degradation profile has a typical pseudo first-order form. However, as predicted by Eqn (2), the k_{app} depends inversely on the Triton concentration. In fact, Eqn (2) has a similar form to the rate law corresponding to an inhibition by an initial product (B) in a two-step reaction ($A - B + C = B + A - C \rightarrow \text{Products}$) in which it has been established^[38] that its occurrence causes a deviation from pseudo first-order kinetics that may not be easily noticeable. Similar consequences are experimentally observed for the case of the L-H reaction rate law given by Eqn (2). Therefore, extreme care must be taken when comparing apparent pseudo first-order rate constants in photocatalytic (TiO_2) processes since their values depend on the reactant concentration as predicted by Eqn (2) and contradict true first-order kinetics. Although k_{app} depends inversely on the $[\text{Triton}]$ (Eqn (1)), the rate = $k_{\text{app}} [\text{Triton}]$ (Eqn (1)), is kept almost constant during the kinetic run since k_{app} increases when decreasing concentration. For instance, it can be seen in

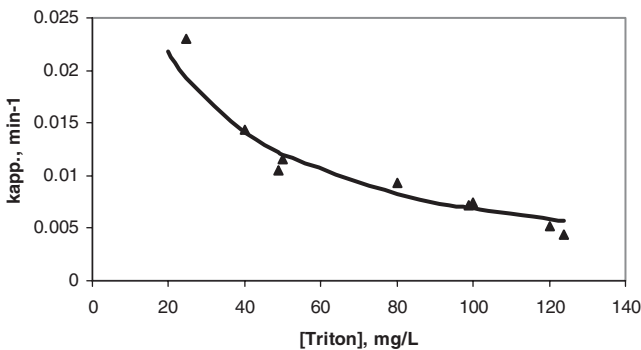


Figure 4. Plot of k_{app} values versus $[\text{Triton}]_0$. Solid line best fit of the experimental points to the equation $k_{\text{app}} = 0.05/(1 + 0.06[\text{Triton}]_0)$. As shown in Eqn (2)

Table 1. Experimental and theoretical k_{app} (min^{-1}) values for Triton X-100 degradation in water

[Triton] (mg L^{-1})	k_{app} (10^{-3} min^{-1}) ^a	R^2 ^b	k_{app} (10^{-3} min^{-1}) ^c	k_{app} (10^{-3} min^{-1}) ^d	rate ($\text{mg L}^{-1} \text{ min}^{-1}$) ^e
24.8	23.0 ± 2.0	0.9948	12.8	19.3	0.32 ± 0.02
40.0	14.3 ± 0.4	0.9960	9.9	14.1	0.37 ± 0.03
48.8	10.5 ± 0.1	0.9907	8.7	12.2	0.44 ± 0.01
50.0	11.6 ± 0.3	0.9970	8.6	12.0	0.44 ± 0.05
80.0	9.3 ± 0.4	0.9940	6.2	8.3	0.56 ± 0.09
99.0	7.2 ± 0.2	0.9494	5.2	6.9	0.45 ± 0.02
100.0	7.4 ± 0.6	0.9720	5.2	6.8	0.56 ± 0.11
120.0	5.2 ± 0.4	0.9720	4.5	5.8	0.51 ± 0.10
124.0	4.4 ± 0.4	0.9788	4.4	5.7	0.56 ± 0.01

Radiation intensity $50 \mu\text{W cm}^{-2}$, amount of TiO_2 used 100 mg L^{-1} , temperature 22°C . Standard deviation corresponds to triplicates.

^a Obtained from the slope of $\ln [\text{Triton}]$ versus time.

^b Linear coefficient from the straight lines.

^c Values obtained using Eqn (2), $k = 0.66 \pm 0.07 \text{ mg L}^{-1} \text{ min}^{-1}$ and $K = 0.037 \pm 0.008 \text{ L mg}^{-1}$ (from $1/v$ vs. [Triton] plot) values (Fig. 3).

^d Values obtained using $k = 0.8 \text{ mg L}^{-1} \text{ min}^{-1}$ and $K = 0.06 \text{ L mg}^{-1}$ from best fitting of the experimental points (Fig. 4).

^e Rates measured from the initial slope of a [Triton] versus t plot at each initial [Triton].

Table 1 that rates (last column) remains very much unchangeable with changes in concentration. We are then dealing with a special case of pseudo-zero order reaction due to the cancellation of the [Triton] term in Eqn (1). k_{app} values are obtained independently from $\ln [\text{Triton}]$ versus t plots but the [Triton] data change as a zero-order reaction (the same slope, in a [Triton] vs. t plot); however, the \ln function, from where the k_{app} values are obtained, define a smooth curve difficult to distinguish from a straight line, moreover, the \ln function changes with less slope (k_{app}) at higher argument ([Triton]), as observed experimentally in the $\ln [\text{Triton}]$ versus t plots.

Although the use of these k_{app} values has limitations, they may be still useful, for instance, in evaluating competition between two or more substrates for the catalytic sites on TiO_2 if the concentration of the reactant to which k_{app} is being measured, is kept fixed in the competition kinetics runs. An example of this application is given in Subsection "photocatalytic degradation of a solution of *p*-nitrophenol in aqueous Triton solutions."

k_{app} and pH

In Table 2 (second column), the k_{app} values at three pH values are shown. From the former values, it can be concluded that the

reaction is accelerated by OH^- with an observed rate constant leveling at pH *ca.* 7. The leveling is consistent with the TiO_2 pH zero point of charge (pH_{zpc}) of 6.8.^[39,40] At pH < 6.8, the TiO_2 surface is positively charged and the interaction with the surfactant or the OH^- is favorable as compared to when pH > 6.8 at which the surface is negatively charged and its interaction either with the surfactant or the OH^- is disfavored. Therefore, at pH > 6.8, the OH^- acceleration is balanced by the unfavorable electrostatic interaction at the catalyst surface and a leveling of the k_{app} value is observed.

At pH < TiO_2 pH_{zpc} , the reaction is catalyzed by $[\text{OH}^-]$; this means that the hydroxyl group plays an important role in the surfactant oxidation mechanism. Indeed, the hydroxyl group is transformed^[11] into a hydroxyl radical by donating an electron to the hole formed at the catalyst by the action of light. These additional radicals promote surfactant degradation.

Triton mineralization (miner.)

Mineralization (transformation into $\text{CO}_2 + \text{H}_2\text{O}$) of Triton was followed by measuring the OCD. From plots of $\ln \text{OCD}$ versus t at pH 4, 7, and 10, the k_{app} (miner.) values shown in Table 2 were obtained. In the same Table, k_{app} values obtained from Triton degradation are also shown. Since $k_{app} > k_{app}$ (miner.) at the pH studied, it is concluded that the mineralization rate-limiting step is not the one corresponding to Triton degradation.

Intermediates identification

Four intermediates (A,B,C, and D; Fig. S2; Supporting Information) were identified using the mass spectra instrument database. Those correspond to: A, *tert*-octylphenol (4-(1,1,3,3)-tetramethylbutylphenol); B, *tert*-octylphenoxyethanol; C, *tert*-octyl phenoxyethyl formate, and D, *tert*-octylphenoxydiethoxyl formate. In Scheme 1 these intermediates are shown. Triton molecule has three functional groups from where degradation can be initiated: *tert*-octyl group, aromatic ring, and the polyethoxyl chain. However, the alkylphenols and the phenoxyethoxyl formate formation constitute evidence to affirm that the

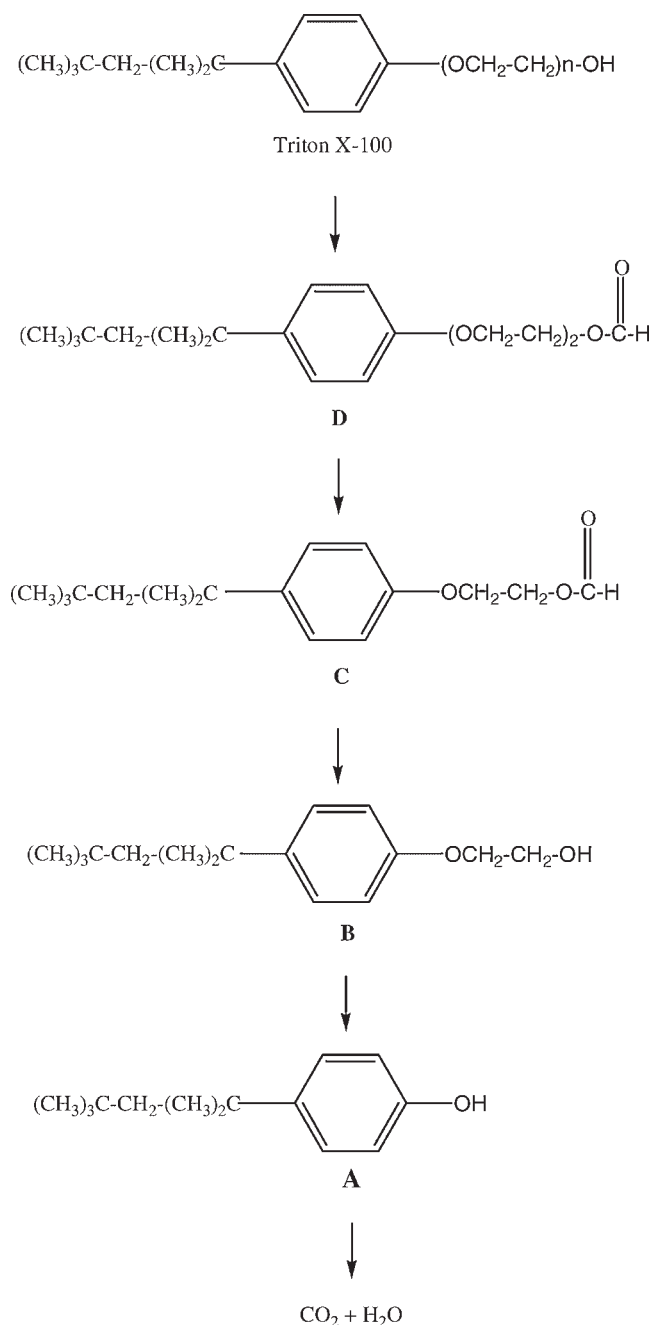
Table 2. k_{app} (degradation) and k_{app} (miner.) (mineralization) of Triton at different pH using water as solvent

pH	k_{app} (10^{-3} min^{-1}) ^a	R^2	k_{app} (miner.) (10^{-3} min^{-1}) ^b	R^2
4	2.7 ± 0.3	0.9927	1.23 ± 0.01	0.9519
7	10.5 ± 0.1	0.9721	1.90 ± 0.02	0.9535
10	9.85 ± 0.07	0.9881	3.48 ± 0.01	0.9758

Radiation intensity $50 \mu\text{W cm}^{-2}$, amount of TiO_2 used 100 mg L^{-1} , temperature 22°C .

^a Triton degradation measured by following Triton disappearance.

^b Triton mineralization from OCD at different reaction times.



Scheme 1. Triton degradation identified intermediates by GC/MS at $t = 180$ min. Conditions: HP-5 column $30\text{ m} \times 0.32\text{ }\mu\text{m}$ internal diameter; eluent gas He, flux 38.1 ml min^{-1} ; injection temperature $240\text{ }^\circ\text{C}$; column temperature at $40\text{ }^\circ\text{C}$ during 4 min and $40\text{--}300\text{ }^\circ\text{C}$ at $10\text{ }^\circ\text{C min}^{-1}$. $[\text{Triton}] = 48.8\text{ mg L}^{-1}$; irradiation intensity $50\text{ }\mu\text{W cm}^{-2}$; $[\text{TiO}_2] = 100\text{ mg L}^{-1}$; pH 4

initial oxidation occurs at the polyethoxylated chain. If the reaction initiation occurs via radical OH attack to the Triton polyethoxyl chain, there are two attacking points on the chain from where different intermediates may be produced. Attack at the first (phenoxy attached) methylene group produces a radical that after reaction with oxygen yields alkoxy radical that can break either a C—C bond to form ethoxyl formate derivative and intermediates **D** and **C** or a C—O bond to yield ethoxylphenol derivative that by OH[·] and O₂ action form intermediates **B** and **A**.

If the hydroxyl attack is on the second methylene group (α to the —OCH₂— group), after interaction with O₂, an alkoxy radicals is produced that suffers a C—C cleavage to yield alkyl radical that forms, after oxygen attack, intermediates **A** and **B**. A similar degradation mechanism has been proposed by Brand^[41] in the Fe (III) photoinduced degradation of Igepal CA 520 (an ethoxyl alkylphenol). It is important to point out that the identified intermediates maintain the aromatic ring in their molecules. Therefore, they contribute to the absorbance of the starting material shown in Fig. 1. So that, their formation may be a cause for the error observed (as shown in Table 1, column 2 vs. column 4) in the k and K values at low Triton, where their relative presence, as compared to the reactants, is more important. Therefore, the obtained k_{app} values are really an average of the faster degradation of these intermediates with a shorter pendant ethoxyl chain and the remaining Triton. Since the rates are evaluated at shorter times (initial rate method) as compared to the rate constants (k_{app}), it is quite possible that the fraction of the intermediates contributes more at the rate constants (k_{app}) than at the rates (r) form where the k and K values are evaluated.

On the other hand, it is the lost of the aromatic ring that contribute to the decrease in the absorbance at 225 nm and to the degradation kinetics. These species could not be identified in the CG-MS spectra, although its formation is detected at short elution time as a broad signal (Fig. S2, Supporting information). The degradation of these stable non-aromatic species might be the rate-limiting step for the mineralization.

Photocatalytic degradation of a solution of *p*-nitrophenol in aqueous Triton solutions

In order to study the surfactant influence on the degradation of organic substrates, we studied *p*-nitrophenol degradation in Triton water solutions. Different Triton concentrations were used keeping the *p*-nitrophenol concentration constant.

Rate constants were obtained from the slope of a $\ln [\text{p-nitrophenol}]$ versus time plot. The results are shown in Fig. 5 and Table 3. As shown, the apparent pseudo first-order rate constants k_{app} decrease when $[\text{Triton}]$ increases. This tendency

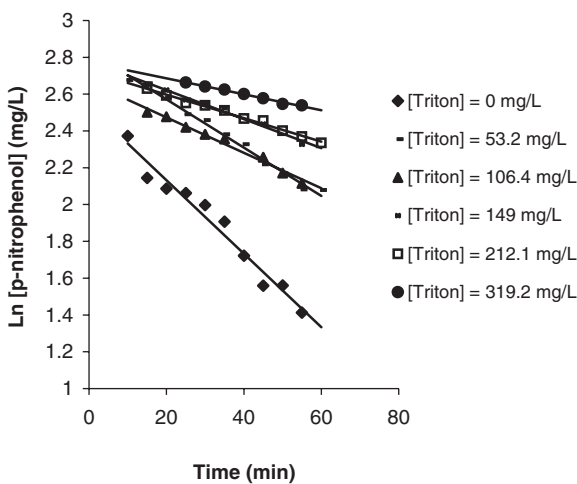


Figure 5. Effect of [Triton] on the *p*-nitrophenol photodegradation. $[\text{p-nitrophenol}]_0 = 13.7\text{ mg L}^{-1}$, $[\text{TiO}_2] = 100\text{ mg L}^{-1}$, radiation intensity $50\text{ }\mu\text{W cm}^{-2}$, pH 7 (water), temperature $22\text{ }^\circ\text{C}$. [TX]Triton, X-100 concentration

Table 3. Values of rate constants (k_{app}) and half-life ($t_{1/2}$) of the *p*-nitrophenol degradation in water at pH 7 at different Triton X-100 concentrations

[Triton], mg L ⁻¹	k_{app} (min ⁻¹)	$t_{1/2}$ (min)	R^2
[Triton] < CMC			
0	0.024 ± 0.003	29 ± 3	0.972
53.2	0.0133 ± 0.0002	52.1 ± 0.8	0.9909
106.4	0.0094 ± 0.0003	74 ± 2	0.9884
150.0	0.0082 ± 0.0003	84 ± 3	0.9834
[Triton] > CMC			
212.8	0.0062 ± 0.0002	112 ± 4	0.9979
319.2	0.0043 ± 0.0003	160 ± 11	0.9903
Radiation intensity 50 μ W cm ⁻² , amount of TiO ₂ used 100 mg L ⁻¹ , temperature 22 °C.			

can be explained in terms of the L-H equation when two substrates compete for the catalyst sites (Eqn (3)).

$$k_{app} = \frac{K'K'}{1 + K'[phenol]_0 + K[Triton]_0} \quad (3)$$

Since $K[Triton]_0 > K'[phenol]_0$ ($K'[phenol]_0 = 0.025 \text{ L mg}^{-1} \times 13.7 \text{ mg L}^{-1} = 0.34$ ^[42]), the induced Triton inhibition is detected in the *p*-nitrophenol k_{app} experimental measurements. As shown in Fig. 6, the experimental k_{app} values have been fitted to Eqn (3), in which $K'K' = 0.032 \text{ min}^{-1}$, $K'[phenol]_0 = 0.34$ and $K = 0.022 \text{ L mg}^{-1}$. The last value is lower than the one obtained directly from Triton degradation (0.037 L mg^{-1} from Fig. 3 and 0.06 L mg^{-1} from best fitting) as a probably consequence of the perturbed TiO₂ surface due to the competing phenol adsorption. The plots shown in Figs. 4 and 6 are very similar. In fact, the plots are identical at high [Triton] in agreement with equal Eqns (2 and 3) denominators (in Eqn (3), $K[Triton]_0 > K'[phenol]_0$). The only difference between the two plots is the initial points since the numerator is different 0.032 (Eqn (3)) versus 0.048 (Eqn (2)).

The low value of the product kK for TiO₂ degradation is very useful in the degradation of water non-soluble petroleum fraction as PAH (polyaromatic hydrocarbons) and asphaltenes.

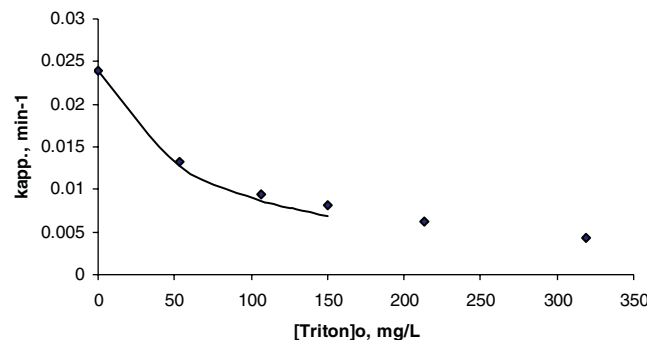


Figure 6. Plot of k_{app} values versus $[Triton]_0$. Solid line best fit of the experimental points to the equation $k_{app} = 0.032/(1 + 0.34 + 0.022 [Triton]_0)$. As shown in Eqn (3). Only the experimental points at $[Triton]_0 < \text{CMC}$ ($\text{CMC} = 150 \text{ mg L}^{-1}$) were used to the best fit. The other two experimental points at $[Triton]_0 > \text{CMC}$, are also shown in the plot

For instance, we have elucidated the optimal experimental conditions to selectively degrade naphthalene in Triton solutions^[28] and we have degraded^[43] conveniently, dibenzophenone (DBT) in presence of Triton.

CONCLUSIONS

A decrease in the Triton degradation rate is observed when $[Triton]_0$ is increased. This result is in agreement with any mechanism that fits the rate law $k_{app} = kK/(1 + K[Triton]_0)$ in which the reaction rate constant depends inversely on Triton initial concentration when $K[Triton]_0 > 1$, but the deviation from pseudo first-order kinetics is not noticeable. This inverse initial concentration dependency is a consequence of the general Langmuir-Hinshelwood (L-H) mechanistic proposal. That is, a fast pre-equilibrium is established between the reactant in solution and the reactant attached to active sites on the TiO₂ surface. Therefore, kinetically equivalent mechanisms with a rate law like the one predicted by the L-H model, will show the inverse initial concentration dependency. In view of this inverse initial concentration dependency, special care must be taken when k_{app} values are used as inhibition criteria or to compare kinetic data. Nevertheless, the k_{app} can be safely used as an inhibition criterion when a competition for the catalyst is established (for instance, *p*-nitrophenol vs. Triton in this study) and the reaction rate is monitored following one of the reactants whose initial concentration is kept constant in all experiments.

Triton initial oxidation occurs at the polyethoxylated chain. Intermediates with shorter ethoxyl chains are formed previous to the degradation rate-limiting step that involves the aromatic ring oxidation.

Acknowledgements

This project was financed by Venezuelan Conipet-Fonacit No. 97-003767 (Consejo Nacional de Investigaciones Petroleras-Fondo Nacional de Ciencia, Tecnología e Investigación), UGA-USB (Unidad de Gestión Ambiental de la Universidad Simón Bolívar), and DID-USB (Decanato de Investigación y Desarrollo de la Universidad Simón Bolívar).

REFERENCES

- [1] M. A. Fox, M. T. Dulay, *Chem. Rev.* **1993**, *93*, 341–357.
- [2] O. Legrini, E. Oliveros, A. M. Braun, *Chem. Rev.* **1993**, *93*, 671–698.
- [3] E. Pelizzetti, *Solar En. Mat. Sol. Cells* **1995**, *38*, 453–457.
- [4] D. F. Ollis, E. Pelizzetti, N. Serpone, *Photocatalysis: Fundamentals and Applications*, Wiley-Interscience, New York, **1989**.
- [5] I. Kuher, O. Núñez, *Pest. Manag. Sci.* **2007**, *63*(5), 491–494.
- [6] H. Hidaka, J. Zhao, E. Pelizzetti, N. Serpone, *J. Phys. Chem.* **1992**, *96*, 2226–2230.
- [7] S. Dube, N. N. Rao, *J. Photochem. Photobiol. A: Chem.* **1996**, *93*, 71–77.
- [8] E. Pelizzetti, C. Minero, V. Maurino, A. Sclafani, H. Hidaka, N. Serpone, *Environ. Sci. Technol.* **1989**, *23*, 1380–1385.
- [9] H. Hidaka, K. Ihara, Y. Fujita, S. Yamada, E. Pelizzetti, N. Serpone, *J. Photochem. Photobiol. A: Chem.* **1988**, *42*, 375–381.
- [10] K. P. Pennel, L. M. Abriola, W. J. Weber, Jr., *Environ. Sci. Technol.* **1993**, *27*, 2332–2340.
- [11] E. C. Butler, K. F. Hayes, *Water Res.* **1998**, *32*(5), 1345–1354.

[12] D. F. Lowe, C. L. Oubre, C. H. Ward, *Surfactants and Cosolvents for NAPL Remediation. A Technology Practices Manual*, Lewis Publisher. Boca Raton, Florida, **1999**.

[13] L. Strbak, In situ flushing with surfactants and cosolvents. *National Network of Environmental Management Studies Follow for USEPA*, July 2000.

[14] S. Guha, P. R. Jaffé, C. A. Peters, *Environ. Sci. Technol.* **1998**, *32*, 930–935.

[15] D. E. Kile, C. T. Chiou, *Environ. Sci. Technol.* **1989**, *23*, 832–838.

[16] E. Pramauro, A. B. Prevot, M. Vicentini, R. Gamberini, *Chemosphere* **1998**, *36*(7), 1523–1542.

[17] USEPA. *Oficina de Innovaciones Tecnológicas. Guía del Ciudadano: El enjuague del suelo in situ*. EPA-542-F-96022, April, **1996**.

[18] A. Núñez, G. Pardo, O. Núñez, Química Sustentable. Tratamiento de Desechos Líquidos de La Industria Petrolera. Nuestra Experiencia en Laboratorio. Universidad Nacional del Litoral (Argentina), **2004**.

[19] T. M. El-Morsi, W. R. Budakowski, A. S. Abd-El-Azis, K. J. Friesen, *Environ. Sci. Technol.* **2000**, *34*, 1018–1022.

[20] S. Malato, J. Blanco, C. Richter, M. I. Maldonado, *Appl. Catal. B: Env.* **2000**, *25*, 31–38.

[21] C. S. Turchi, D. F. Ollis, *J. Catal.* **1990**, *122*, 178–192.

[22] M. Ranchella, C. Rol, G. V. Sebastián, *J. Chem. Soc. Perkin Trans.* **2000**, 311–316.

[23] K. B. Dhanalakshmi, S. Anandan, J. Madhavan, P. Maruthamuthu, *Sol. Energ. Mater. Sol. Cell.* **2008**, *92*, 457–463.

[24] A. Ortiz-Gomez, B. Serrano-Rosales, M. Salaices, H. De Lasa, *Ind. Eng. Chem. Res.* **2007**, *46*, 7394–7409.

[25] F. Arsac, D. Bianchi, J. M. Chovelon, C. Ferronato, *J. Phys. Chem. A* **2006**, *110*, 4213–4222.

[26] A. V. Emeline, V. Ryabchuk, N. Serpone, *J. Photochem. Photobiol. A* **2000**, *133*, 89–97.

[27] S. Brosillon, L. Lhomme, C. Vallet, A. Bouzaza, D. Wolbert, *Appl. Catal. B* **2008**, *78*, 232–241.

[28] N. Barrios, P. Sivov, D. D'Andrea, O. Núñez, *Int. J. Chem. Kinetics* **2005**, *7*(37), 414–419.

[29] S. Nevim, A. Htipoglu, G. Koctürk, Z. Cinar, *J. Photochem. Photobiol. A: Chem.* **2002**, *146*, 189–197.

[30] H. Al-Ekabi, N. Serpone, *J. Phys. Chem.* **1988**, *92*, 5726–5731.

[31] M. Trillas, M. Pujol, X. Domenech, *J. Chem. Technol. Biotechnol.* **1992**, *55*, 85–90.

[32] J. M. Winterbottom, Z. Khan, A. P. Boyes, S. Raymahasay, *Environ. Prog.* **1997**, *62*, 125–131.

[33] J. Tseng, C. P. Huang, Mechanistic aspects of photocatalysis oxidation of phenol in aqueous solutions. in *Emerging Technologies in Hazardous Waste Management* (Eds.: D. W. Tedder, F. G. Pollard), ACS, Washington, D.C, **1990**. Chapter 2.

[34] W. Boyles, *The Science of Chemical Oxygen Demand, Technical Information Series, Booklet No. 9*. Hach Company, USA, **1997**.

[35] M. Franson, *Métodos normalizados para el análisis de aguas potables y residuales* 1st edn, Editorial Diaz Santos, España, **1992**.

[36] R. W. Matthews, *Water Res.* **1990**, *24*(5), 653–660.

[37] R. W. Matthews, *J. Phys. Chem.* **1987**, *91*, 3328–3333.

[38] W. P. Jencks, *Catalysis in Chemistry and Enzymology*, McGraw Hill, USA, **1969**.

[39] J. Zhao, K. Wu, T. Wu, H. Hidaka, N. Serpone, *J. Chem. Soc. Faraday Trans.* **1998**, *94*(5), 673–676.

[40] J. Zhao, H. Hidaka, A. Takamura, E. Pelizzetti, N. Serpone, *Langmuir* **1993**, *9*, 1646–1650.

[41] N. Brand, G. Mailhot, M. Bolte, *Environ. Sci. Technol.* **1998**, *32*(18), 2715–2720.

[42] M. A. Martínez, A. Núñez, R. López, F. Morales, O. Núñez, *Acta Cient. Venez.* **1999**, *50*(1), 81–86.

[43] R. Vargas, O. Núñez. The Photocatalytic Oxidation of Dibenzothiophene (DBT). *J. Mol. Cab. A. Chem.* **2008**. [in press].